PHYSICAL REVIEW B **68**, 064409 (2003)

Magnetization of the unsegregated and segregated (100) surface of MoV binary alloys

A. V. Ponomareva,[1] L. V. Pourovskii,[2] E. I. Isaev,[1] Y. Kh. Vekilov,[1] B. Johansson,[2,3] and I. A. Abrikosov[2]
[1]*Theoretical Physics Department, Moscow Steel and Alloys Institute, 117419, 4 Leninskii pr., Moscow, Russia*
[2]*Condensed Matter Theory Group, Physics Department, Uppsala University, Box-530, S-75121 Uppsala, Sweden*
[3]*Applied Material Physics, Department of Material Science and Engineering, Royal Institute of Technology, SE-10044 Stockholm, Sweden*

(Received 23 December 2002; revised manuscript received 14 April 2003; published 7 August 2003)

By means of *ab initio* electronic structure calculations we have investigated the magnetic properties of the (100) surface in the body-centered-cubic (bcc) V-Mo system. Calculations have been carried out for pure V, for uniformly random $Mo_{25}V_{75}$, $Mo_{50}V_{50}$, and $Mo_{75}V_{25}$ binary alloys, as well as for alloys with a self-consistent segregation profile, and for V overlayers deposited on Mo substrate. While the MoV alloy is nonmagnetic in the bulk for the whole interval of concentrations, we predict a noticeable magnetization to occur in the top layer at the (100) surface. The surface segregations essentially enhance the surface magnetization of V for Mo-rich alloys. The largest and most stable magnetic moment is predicted for the case of a single V monolayer deposited on a Mo (100) surface. The origin of the surface magnetization is explained in terms of the electronic structure of the surface alloy.

DOI: 10.1103/PhysRevB.68.064409 PACS number(s): 75.70.Rf

I. INTRODUCTION

Due to the importance of magnetic devices for modern technology, there is a constant need for new magnetic materials. This led to discoveries of new phenomena such as the oscillatory magnetic interlayer coupling in superlattices and multilayers,[1,2] which show the giant magneto resistance (GMR) effect.[3] New classes of materials are synthesized, like, for example, magnetic semiconductors.[4] One avenue for the search for artificial magnetic materials is the possibility of making nonmagnetic transition metals to become magnetic via reducing the dimensionality of the system. Indeed, it is well established theoretically that by reducing the number of the nearest neighbors for a given atom one may increase the magnetic moment in the system.[5] Therefore, low-dimensional systems like nanoclusters, thin films, and surfaces represent an attractive class of objects for the search for new magnetic materials.

In particular, one may expect that some metals like Pd, V, and Rh, which are ''almost ferromagnetic'' in the bulk could become magnetic at the surface. Though the surfaces of Pd and Rh appeared to be nonmagnetic,[6–9] the magnetic properties of the V (100) surface or its interfaces with other materials attracted the attention of researchers during the last 25 years. Contradictory results have been reported so far by both experimentalist[10–14] and theoreticians.[15–20]. Unfortunately, the sensitivity of the magnetic measurements to external conditions, for example, contamination of the surface,[13] as well as theoretical calculations of their details[17–20] does not allow one to reach a conclusion regarding the possibility to magnetize surface V atoms. At the same time, thin films of nonmagnetic transition metals can also become magnetic. In some systems a noticeable magnetization has been predicted for monolayer films deposited on nonmagnetic, e.g., noble, metals,[9,21–23] though those results are difficult to check experimentally.[24–26] Magnetism is predicted for free and supported V clusters[27] and at vicinal surfaces of vanadium.[28] Still, to the best of our knowledge, no definite confirmation of V to become magnetic is obtained.

Recently, Turek *et al.*[29] have suggested another way to search for V magnetism; i.e., they suggested to consider surfaces of transition-metal alloys. Turek *et al.* have carried out first-principles electronic structure calculations for the (100) surface of the disordered bcc RuV, RhV, and PdV alloys in a wide range of concentrations. While the alloys are still nonmagnetic in the bulk and the (100) surfaces of pure V, Ru, Rh, and Pd were also found to be nonmagnetic, the (100) alloy surfaces are predicted to become magnetic and the calculated average magnetic moments reach $(0.6–0.8)\mu_B$ for vanadium-rich alloys. As has been correctly pointed out by the authors themselves, a number of crucial simplifications have been employed in their calculations. In particular, possible deviations of the surface composition from the bulk concentration due to surface segregations have not been taken into account self-consistently, and the influence of atomic ordering at the surface on the surface magnetism has been neglected. Moreover, the RuV, RhV, and PdV alloys form stable disordered bcc solid solutions only for V-rich compositions, and the temperatures of order-disorder phase transitions, which occur in all three systems, are quite high.[30] Therefore, it is going to be difficult to obtain experimental confirmation of the results reported in Ref. 29. For example, theoretical calculations for the (100) surface of bcc PdV alloy with a self-consistent segregation profile predict that it is nonmagnetic.[31]

Apparently, the origin of the problem mentioned above is that V has higher surface energy than Pd.[32,33] As a matter of fact, the stability of V films on the noble-metal substrates should be poor due to the same problem. Therefore, one may try to search for an alloying element with the surface energy that is closer to or even higher than that of V.[34] In the present paper we propose to alloy V with Mo, which indeed has a higher surface energy.[32,33] The nonmagnetic-in-bulk alloy, according to our calculations, should then have the (100) surface enriched with V and it should be magnetic. The bcc MoV disordered solid solution is stable in the whole interval of concentrations, and no ordering takes place in the system. We have carried out an *ab initio* investigation of the magnetic properties of the (100) surface for the $\mathrm{Mo}_{25}\mathrm{V}_{75}$, $\mathrm{Mo}_{50}\mathrm{V}_{50}$, and $\mathrm{Mo}_{75}\mathrm{V}_{25}$ disordered bcc alloys using the coherent potential approximation (CPA) and interface Green's function (GF) linear muffin-tin orbital method within the atomic-sphere approximation with multipole corrections (LMTO-ASA+M).[35–37] We have studied the magnetization of both uniformly random and segregated surfaces. In order to find the equilibrium segregation profile for the (100) surface we have employed a recently developed technique[38] which uses the Ising-like Hamiltonian with effective interatomic interactions derived from first principles by means of the screened generalized perturbation method[39] (SGPM) and the direct exchange Monte Carlo (DEMC) method[40] for statistical mechanics simulations of the surface structure.

The present paper is organized as follows. In Sec. II details of our calculations are presented. In Sec. III we present our results, including the calculations for pure V, the calculated magnetic moments at the (100) surface of uniformly random MoV alloys, the calculated equilibrium segregation profiles, magnetization of the segregated (100) surface, and the magnetization of V monolayer deposited on Mo.

II. DETAILS OF THE CALCULATIONS

The bcc (100) Mo-V surface was treated in the semiinfinite geometry within the GF technique and the LMTO-ASA+M method. Bulk and supercell calculations were also carried out by means of the same technique. The method was described in details in Refs. 35–37, and here we only outline the relevant parameters for our calculations. The basis functions have been truncated at $l_{max}=3$ and the multipole moments expansion was carried out up to $2l_{max}+1$. The Vosko-Wilk-Nusair approximation[41] has been employed for the exchange-correlation energy and potential. The Brillouin zone (BZ) integration has been carried out using 505 *k* points distributed over the irreducible part of the bcc Brillouin zone in bulk and 136 *k* points distributed over the irreducible part of the two-dimensional Brillouin zone for the (100) surface. Energy integration has been carried out in the complex plane on a semicircular contour comprising 24 energy points. Because energy differences between ferromagnetic and nonmagnetic solutions were often quite small, we used the fixed spin moment method, described in details in Ref. 42.

In order to calculate equilibrium segregation profiles the surface energy E_{tot}^{surf} was mapped onto the effective Ising-like Hamiltonian:

$$E_{tot}^{surf}=V^{(0)}+\sum_{\lambda}\left[V_{\lambda}^{(1)}\langle\sigma_{\lambda}\rangle+\sum_{\lambda',s}V_{\lambda\lambda'}^{(2,s)}\langle\sigma_{\lambda;i}\sigma_{\lambda';j}\rangle_{s}+\cdots\right], \tag{1}$$

where the spin variables σ_i take on values $+1$ or -1 depending on the type of atom occupying site *i*. The average products of the spin variables, $\langle\sigma_i\sigma_j\cdots\sigma_k\rangle$, are the multisite correlation functions which form a complete basis for the total energy expansion,[43] the effective interactions $V_{\lambda\lambda'\lambda''}^{(d,s)}\cdots$ depend on the cluster order *d* and its type *s*, and on the relative position of the cluster $\lambda\lambda'\cdots$, which designates those atoms of the cluster that are located in layers λ, λ', λ'', and so on.[44] The multisite potentials $V_{\lambda\lambda'''\lambda}^{(d,s)}\cdots$ have been calculated using the SGPM method,[39] and on-site interactions $V_{\lambda}^{(1)}$ have been obtained by differentiation of E_{tot}^{surf} of an equviatomic alloy surface with respect to the layer concentration:

$$V_{\lambda}^{(1)}=\left.\frac{dE_{tot}^{surf}}{d\langle\sigma_{\lambda}\rangle}\right|_{\langle\sigma_{\lambda}\rangle=0}-\left.\frac{dE_{tot}^{surf}}{d\langle\sigma_{\lambda_b}\rangle}\right|_{\langle\sigma_{\lambda_b}\rangle=0}, \tag{2}$$

where λ_b designates a layer in bulk or, in practice, a layer located far enough from the surface so the surface influence on it is negligible. Expression (2) is similar to the definition of the segregation energy, but on-site potentials $V_{\lambda}^{(1)}$ are calculated at 50% alloy concentration in order to single out contributions to the on-site potential from pair and higher-order interactions. At the same time the volume in Eq. (2) is chosen equal to the equilibrium volume for a given alloy concentration. It is important to notice that the formalism presented in Ref. 43 is developed for concentration-independent interactions, while SGPM effective potentials are concentration dependent. However, one can easily transform concentration-independent interactions into concentration-dependent ones using a simple relationship derived in Ref. 45. The SGPM effective potentials have been calculated using a 16-layer tetragonal supercell (11 layers of alloy and 5 layers of vacuum), and the Brillouin zone integration in this case has been performed using 180 *k* points in the irreducible part of the Brillouin zone. Due to a moderate charge transfer between components in MoV alloys (0.3 electrons/atoms), the electrostatic contribution to the effective potentials is small, and we have neglected it in our simulations.

Equilibrium surface segregation profiles at finite temperatures were calculated by means of the DEMC method.[38,40] In the DEMC method a sequence of atom exchanges is performed between a surface Monte Carlo (MC) sample and a previously equilibrated bulk MC reservoir. It can be shown[40] that the method is equivalent to the grand canonical ensemble MC method, but generally DEMC is more computationally efficient. As the bulk reservoir we have used a 32 768-atom bcc rigid lattice box ($32\times32\times32$) with periodic boundary conditions. We started with randomly distributed Mo and V atoms at a temperature 2000 K; then the temperature was subsequently lowered by 50 K. In order to reach an equilibrium distribution of atoms in the reservoir 3000 exchange attempts per atom have been made at each temperature, and the total energy, pair correlators, and structure factors were averaged over the last 750 steps per atom. The (100) surface has been simulated by a cell with a surface area 32×32 and a thickness of 28 layers; the number of exchange attempts and initial temperature are the same as in the bulk case.

Because of the small difference in atomic sizes between Mo and V atoms, local relaxations are not expected to give an essential contribution to the alloy total energy, so we have neglected the local relaxations. The effect of surface relaxations was investigated for the case of a V monolayer deposited on a (100) Mo substrate. Note that for the determination of relaxed geometries one needs to go beyond the ASA and to use full-potential techniques. Therefore, we carried out these calculations using the supercell technique and all-electron projector-augmented-wave (PAW) potential as implemented in the VASP code.[46–48] The surface was simulated by means of a slab containing 13 atomic and 4 vacuum layers. Integration over the BZ was done using 384 tetrahedra with Blöchl's corrections.[49] The convergence criterion for the electronic subsystem was chosen to be equal to 10^{-4} eV for two subsequent iterations, and the ionic relaxation loop within the conjugated gradient method was stopped when forces became of the order of 10^{-3} eV/Å.

III. RESULTS AND DISCUSSION

A. (100) surface of pure bcc V

First, we have calculated electronic structure and magnetic moments for the (100) surface of pure bcc V. In agreement with earlier all-electron calculations,[15–18,20,29] we find that V is nonmagnetic at the surface, as well as in the bulk. The calculated local densities of states (LDOS) for the bulk V, as well as for the top layer at the V (100) surface, are displayed in Fig. 1. In agreement with earlier calculations,[29] we see that the surface DOS is narrowed as compared to the bulk due to the reduced coordination number of an atom at the surface, and the center of gravity of the band is shifted towards the lower energies, as expected for elements with less than half-filled *d* band.[50] The most remarkable feature seen in Fig. 1 is the appearance of surface states inside the bulk pseudogap just above the Fermi energy E_F.

In order to relate the magnetic properties and the electronic structure of transition metals one may use the Stoner model, which predicts a metal to become magnetic when the following condition is fulfilled:

$$|I|n(E_F)>1, \tag{3}$$

where $|I|$ is the so-called Stoner parameter and $n(E_F)$ is the density of states at the Fermi level for the metal in the nonmagnetic state. The Stoner parameter is an intra-atomic quantity, which depends weakly on the crystal environment of an atom, and it can be easily evaluated from the results of bulk LMTO-ASA calculations.[51] In our calculations the obtained Stoner parameter for V was found to be equal to 0.031 Ry.

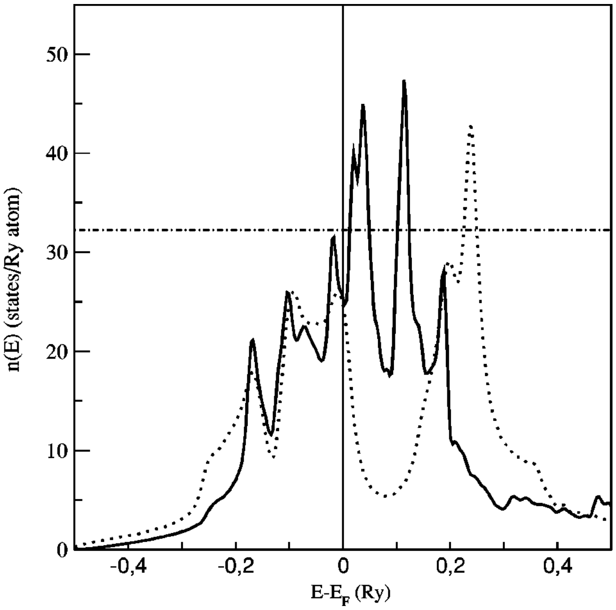

FIG. 1. Calculated density of states $n(E)$ as a function of energy E (relative to the Fermi energy E_F) of pure bcc V in the bulk (dotted line) and for the top layer at the (100) surface (solid line). The dot-dashed horizontal line indicates the value of the inverse Stoner parameter for vanadium.

In Fig. 1 the dot-dashed horizontal line indicates the value of the inverse Stoner parameter $|I^{-1}|$ for vanadium. Thus, if $n(E_F)>|I^{-1}|$, the surface should become magnetic. One may see that for the surface atom at (100) surface of pure V the Fermi level appears just below the high peak, which corresponds to 3*d* surface states. Therefore, if more electrons are added to the vanadium *d* band, the Fermi energy should rise, followed by a sharp increase of the density of states at

TABLE I. Layer-resolved local magnetic moments on V and Mo atoms, as well as net magnetic moments per layer (in μ_B) for ferromagnetic samples, disordered local moments on V atoms (V_{DLM} in μ_B), and energy differences between the ferromagnetic and the nonmagnetic solutions ΔE_{FM-NM} and between the ferromagnetic solution and the solution with a local moment disorder ΔE_{FM-DLM} (in mRy) for uniformly random Mo-V alloys at the (100) surface. Layers are numbered starting with the surface layer S, and decreasing numbers correspond to deeper subsurface layers.

Alloy	Layer	V	V_{DLM}	Mo	Net moment	ΔE_{FM-NM}	ΔE_{FM-DLM}
$Mo_{25}V_{75}$	S	0.91	±0.7	0.19	0.73		
	S-1	−0.12	±0.01	−0.09	−0.10	−0.66	−0.63
	S-2	−0.06	0.00	−0.007	−0.01		
$Mo_{50}V_{50}$	S	1.33	±0.9	0.21	0.77		
	S-1	−0.12	±0.01	−0.09	−0.10	−0.87	−0.78
	S-2	−0.03	0.00	−0.01	−0.01		
$Mo_{75}V_{25}$	S	1.51	±1.23	0.23	0.55		
	S-1	−0.09	±0.04	−0.06	−0.07	−0.74	−0.68
	S-2	0.01	±0.01	0.01	0.01		

the Fermi level. The increase of the *bulk* band filling can be achieved by alloying vanadium with a transition metal with a higher *d*-band filling. We suggest to alloy V with Mo. Mo has bcc crystal structure and forms a solid solution with V in a complete interval of concentrations. Moreover, Mo and V belong to neighboring groups in the periodic table of elements. Therefore, we expect that the deformation of the *d* band of the alloy is going to be minimal, as compared to *d* bands of pure elements in the bcc structure. Thus, the main effect of adding Mo to V should be the increased filling of the common bulk *d* band, which should bring the Fermi energy to the peak of the surface DOS, associated with the surface states mentioned above.

B. (100) surface of uniformly random bcc V-Mo alloys

We have calculated magnetic moments for the (100) surface of uniformly random $Mo_{25}V_{75}$, $Mo_{50}V_{50}$, and $Mo_{75}V_{25}$ disordered alloys. By uniformly random alloys we mean alloys where the concentration at the surface and in the near-surface region is exactly the same as in the bulk. That is, there are no surface segregations in the systems. Calculations were performed at the theoretical equilibrium bulk lattice parameters for the corresponding alloys. All three MoV alloys appeared to be nonmagnetic in the bulk at the theoretical equilibrium volume. The obtained magnetic moments for V and Mo, as well as the average moments, are displayed in Table I. Results are given for the three top surface layers. One may see that the top layers for all three alloys are magnetic, and the magnetization is mainly due to V atoms. The V magnetic moment increases with decreasing V concentration, while the average magnetic moment per atom reduces from the $Mo_{25}V_{75}$ alloy to the $Mo_{75}V_{25}$ alloy due to lower vanadium content. Also the magnetization drops by an order of magnitude in the second layer near the surface and it almost completely disappears in the third layer. So one may suppose that the magnetic moments in the subsurface layers are induced by magnetization in the top surface layer. Note that the magnetic moments in these layers are coupled antiparallel to the moments in the surface layer due to the tendency towards antiferromagnetism for elements with a nearly half-filled band. The planar antiferromagnetic structure was obtained for uniformly random RuV, PhV, and PdV alloys in Ref. 29. It was also expected for the surface of pure V, if it was magnetic.[18–20]

The electronic structure calculations confirm our original suggestion regarding the evolution of the alloy DOS upon alloying of V with Mo. The calculated LDOS for nonmagnetic vanadium atoms at the (100) surface and the total bulk DOS of the nonmagnetic alloys $Mo_{25}V_{75}$, $Mo_{50}V_{50}$, and $Mo_{75}V_{25}$ are displayed in Fig. 2. Note that the contribution of Mo to the density of states at E_F is much smaller than the V contribution. Thus, we do not discuss the Mo LDOS. One may see that with increasing Mo concentration the occupation of the *d* band increases, which is reflected by the downwards shift of the bulk DOS relative to the Fermi energy. The surface-state peak is pinned in the bulk pseudogap, and therefore it shifts more and more towards the Fermi level, increasing $n(E_F)$ for surface V atoms. In Fig. 2 one sees that for all uniformly random alloys considered in this study the Stoner criterion is fulfilled.

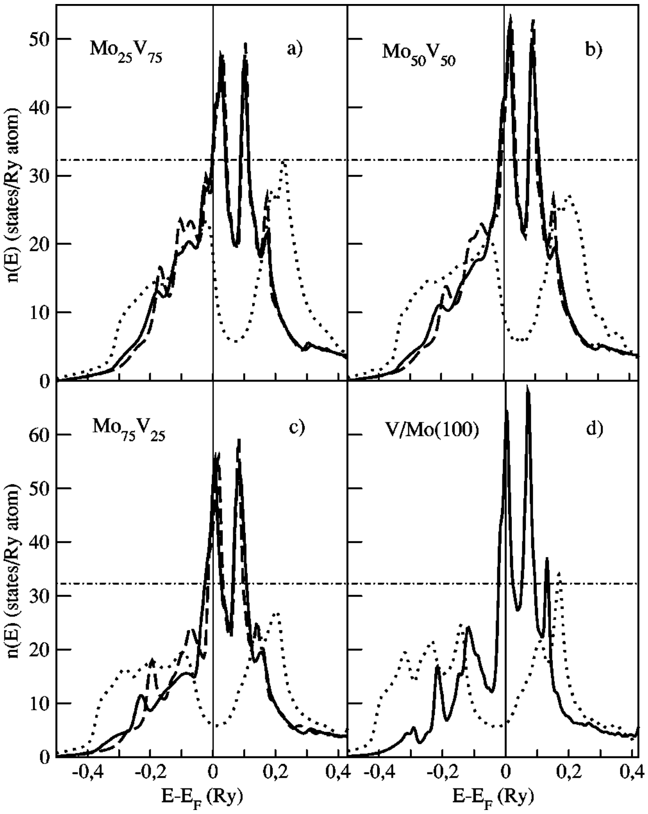

FIG. 2. Vanadium local densities of states $n(E)$ for the top layer at (100) surface of the nonmagnetic bcc (a) $Mo_{25}V_{75}$, (b) $Mo_{50}V_{50}$, and (c) $Mo_{75}V_{25}$ alloys, as well as (d) for the V overlayer deposited on the pure Mo. The LDOS is plotted as a function of energy E (relative to the Fermi energy E_F). The LDOS for the uniformly random alloys is shown with solid lines; the LDOS for alloys with self-consistent segregation profile (quenched from temperature 500 K) is given by long dashed lines. The total bulk DOS for alloys at corresponding concentrations are indicated with dotted lines. The dot-dashed horizontal line indicates the value of the inverse Stoner parameter for V.

The stability of the magnetic solution can be estimated from total energy calculations. In particular, the energy differences between the ferromagnetic (FM) (in the surface plane) solution and the nonmagnetic solution, $\Delta E_{FM} - E_{NM}$, characterize the stability of local magnetic moments, while the one between the FM solution and the solution with a local moments disorder (DLM), $\Delta E_{FM} - E_{DLM}$, may be used as a characteristic of the stability of the FM order in the surface plane. The DLM energies and magnetic moments can be calculated within the CPA assuming that half of all atoms have spin-up moments and the other half have spin-down moments. In Table I we present our results for $\Delta E_{FM} - E_{NM}$. From the table it is seen that this energy difference is in fact rather small for all concentrations, indicating that the FM is not very stable at surfaces of uniformly random alloys. If the FM order is destroyed and the local moments are completely disordered, their magnitude de-

TABLE II. Segregation energies E_{segr} (in mRy) of the V atom towards the (100) surface of uniformly random $\mathrm{Mo}_x\mathrm{V}_{1-x}$ alloys with concentrations 25, 50, and 75 at. % of Mo, assuming three different magnetic states of the alloys: the nonmagnetic (NM), ferromagnetic (FM), and disorder local moments (DLM).

Composition	E_{segr}^{NM}	E_{segr}^{FM}	E_{segr}^{DLM}
$\mathrm{Mo}_{25}\mathrm{V}_{75}$	−31.5	−31.5	−30.9
$\mathrm{Mo}_{50}\mathrm{V}_{50}$	−32.1	−32.4	−29.9
$\mathrm{Mo}_{75}\mathrm{V}_{25}$	−54.5	−61.5	−58.4

TABLE III. The effective on-site potentials $V_\Lambda^1 - V_{bulk}$ (in K) for (100) surface of Mo-V alloys.

	Layers			
Composition	1	2	3	4(bulk)
$\mathrm{Mo}_{25}\mathrm{V}_{75}$	−1438	−515	−941	0
$\mathrm{Mo}_{50}\mathrm{V}_{50}$	−2275	−371	−813	0
$\mathrm{Mo}_{75}\mathrm{V}_{25}$	−3049	−332	−809	0

creases somewhat (see Table I). Note that $\Delta E_{FM} - E_{DLM}$ is very close to $\Delta E_{FM} - E_{NM}$, and therefore the DLM solution is almost degenerate with the nonmagnetic solution. In summary, one cannot expect that the Curie temperature would be high. This can be understood as follows. Though the V density of states at the Fermi level increases with decreasing V concentration, Fig. 2, the dilution effect leads to an increase of nonmagnetic surrounding for each surface V atom, reducing the stability of the FM solution.

Thus, according to our calculations, V atoms at the surface of uniformly random MoV alloys should be magnetic, but the Curie temperature is probably quite low. However, it is unlikely that such a surface can be prepared in practice, because the segregation energies, shown in Table II, are rather big. In the following we study the effect of surface segregation on the magnetic properties of MoV alloys.

C. Surface-concentration profiles at (100) surface of MoV alloys

Equilibrium concentration profiles at temperatures 500 and 1500 K were calculated by means of DEMC simulations with first-principles effective interatomic interactions obtained by means of the SGPM method and one-site potentials (or segregation energies) obtained by a direct differentiation of the surface energy with respect to surface concentration.[38–40] Here we would like to point out that the interplay between the magnetism and phase stability may lead to substantial difficulties. Indeed, the particular structure of an alloy coming out as a result of *ab initio* calculations may be completely different in the paramagnetic (nonmagnetic) and ferromagnetic cases.[52] At the same time, we do not know what magnetic structure would be present in our system at a particular temperature. Therefore, we calculated segregation energies in three uniformly random alloys with concentrations of 25, 50, and 75 at. % of Mo, assuming three different magnetic states of the alloys, the NM, FM, and DLM. Results are shown in Table II. One can see that in our case the calculated segregation energies depend only slightly on the magnetic state. Therefore, all interatomic interactions used for the calculations of the segregation profiles were determined for the nonmagnetic alloys.

The effective interatomic SGPM pair potentials have been calculated up to the 13 coordinational shell. The obtained interatomic potentials are quite small in magnitude. By far the biggest one is a pair potential at the first coordination shell, and it is equal to 290 K. The multisite effective potentials are negligible, so only the pair potential at the first coordinational sphere has been included in the MC simulations. The positive value of the potential favors ordering, but because of its moderate magnitude, no ordering has been observed in our bulk MC simulations down to temperatures of 200 K. This result is in agreement with the experimental bulk phase diagram.[30] Due to weak interatomic interactions in the MoV system, one-site potentials are by far the most important and they determine the shape of the concentration profiles. The on-site potentials in the near-surface region $V_\lambda^{(1)}$ for the $\mathrm{Mo}_{25}\mathrm{V}_{75}$, $\mathrm{Mo}_{50}\mathrm{V}_{50}$, and $\mathrm{Mo}_{75}\mathrm{V}_{25}$ alloys are given in Table III. We assume that the potentials in the first three layers are perturbed by the surface, while the potentials in deeper layers are equal to the bulk value V_{bulk}. Note that the values in Table III are given relative to V_{bulk}. In the effective Hamiltonian (1) we suppose that $\sigma_i = 1$ corresponds to a V atom and $\sigma_i = -1$ corresponds to a Mo atom. One can see that the one-site potentials favor V segregation to the first three layers of the (100) surface. This can be attributed to the lower surface energy of V in comparison with Mo.[33] Analyzing $V_\lambda^{(1)}$, one can also see that the tendency for V segregation increases with decreasing V concentration in the bulk. Some tendency of V to segregate in the second and third layers of the (100) surface can be explained by the quite open character of this surface in bcc crystals. Therefore, the second-third subsurface layers can still "feel" the presence of the surface.

The calculated segregation profiles are displayed in Fig. 3 for temperatures 500 and 1500 K. There are strong V segregations towards the surface layers. In fact, the surfaces are almost completely covered by V for all three alloys considered in the present study. As expected, the oscillations of the segregation profiles increase with decreasing temperature. The oscillations are caused by oscillating values of the one-site potential (see Table III).

D. Magnetization of the segregated (100) surface

Using the self-consistent segregation profiles discussed above we have calculated the surface magnetization for the segregated (100) surface. We assume that the samples are quenched from high temperatures. Thus, our zero-temperature electronic structure calculations have been carried out for the surface segregation profiles obtained at temperature 500 K. The calculated local and average magnetic moments are presented in Table IV. One may see that the net surface magnetization is reduced by the segregations in the case of the $\mathrm{Mo}_{25}\mathrm{V}_{75}$ alloy, while the net magnetization is somewhat enhanced in the case of the $\mathrm{Mo}_{50}\mathrm{V}_{50}$. Moreover, it

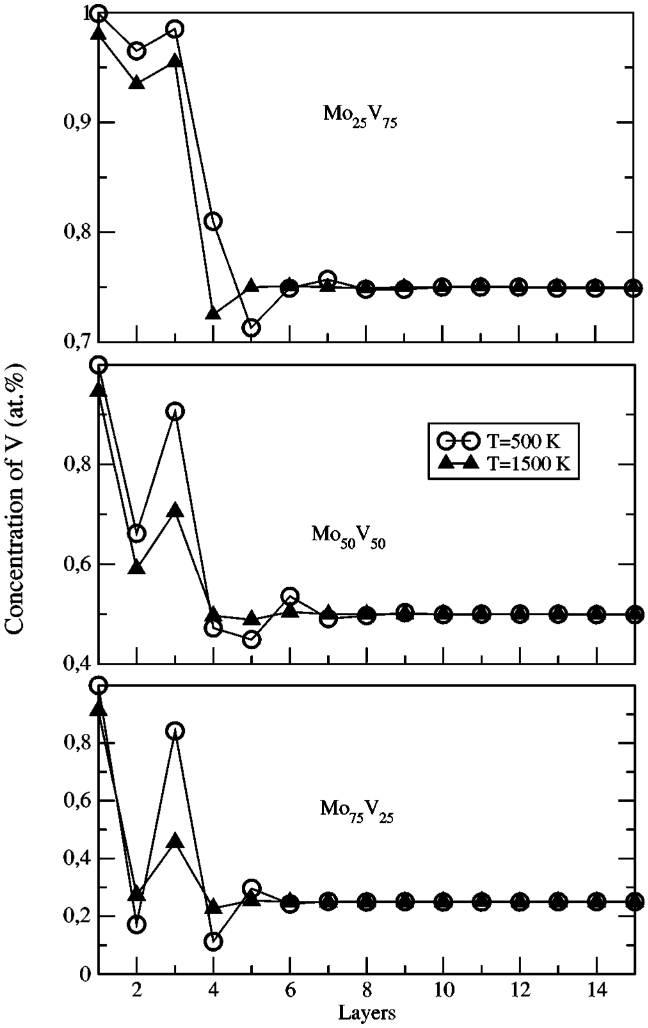

FIG. 3. The surface segregation profiles for the (100) surface of bcc $Mo_{25}V_{75}$ (top panel), $Mo_{50}V_{50}$ (middle panel), and $Mo_{75}V_{25}$ (bottom panel) alloys. The circles and triangles indicate the profiles for temperatures 500 K and 1500 K, respectively. The surface layer is denoted as layer 1, and increasing numbers correspond to deeper layers in the near-surface region.

is strongly (more than twice) enhanced for the $Mo_{75}V_{25}$ alloy. Note that local moments on V atoms decrease a little as compared to the case of the uniformly random alloys (compare Tables I and IV). But the strongly increased V concentration at the surface leads to a substantial increase of the total surface magnetization for Mo-rich alloys. Therefore, the behavior of the surface magnetization can be attributed to the V segregation towards the top layer.

The examination of the local DOS on V atoms at the segregated surface indicates that the surface states, which give rise to the high peaks of the DOS inside the bulk pseudogap, are still present; see Fig. 2. Note that the figure shows the local DOS on V atoms rather than the total DOS. Because of this, the dilution effect that takes place in uniformly random alloys cannot be seen in Fig. 2. With this in mind, we would like to point out that surface segregations have little effect on the shape and height of the peaks, and the DOS at the Fermi level is again above the inverse Stoner parameter at all bulk concentrations considered by us, though it is somewhat lower compared to that of the corresponding uniformly random alloys. This agrees with the small lowering of the local moments on V atoms mentioned above. At the same time, the surface V concentration is high at all bulk compositions, and the dilution effect, which reduces the stability of the FM solutions for the uniformly random alloys, does not play any role for the segregated samples. This allows one to expect that the surface segregation may, in fact, increase the stability of the ferromagnetic solution. Indeed, our total energy calculations confirm this suggestion. For alloys with bulk Mo concentration larger than 50 at. % the energy differences between the ferromagnetic and the nonmagnetic solutions, $\Delta E_{FM} - E_{NM}$, presented in Table IV are substantially more negative than the corresponding values presented in Table I for the surfaces of uniformly random alloys. Segregations also stabilize the FM solution with respect to the DLM solution, as one can see from Table IV, where we show the energy differences between the FM and DLM solutions, $\Delta E_{FM} - E_{DLM}$. As a matter of fact, for alloys with high Mo concentration these energy differences are

TABLE IV. Layer-resolved local magnetic moments on V and Mo atoms, as well as net magnetic moments per layer (in μ_B) for ferromagnetic samples, disordered local moments on V atoms (V_{DLM} in μ_B), and energy differences between the ferromagnetic and the nonmagnetic solutions ΔE_{FM-NM} and between the ferromagnetic solution and the solution with a local moments disorder ΔE_{FM-DLM} (in mRy) for random Mo-V alloys at (100) surface with segregation profiles quenched from temperature $T = 500$ K. Layers are numbered starting with the surface layer S, and decreasing numbers correspond to deeper subsurface layers.

	Layer	V	V_{DLM}	Mo	Total moment	ΔE_{FM-NM}	ΔE_{FM-DLM}
$Mo_{25}V_{75}$	S	0.42	±0.40	-	0.42		
	S-1	−0.12	±0.01	−0.06	−0.11	−0.44	−0.24
	S-2	−0.05	0.00	−0.002	−0.05		
$Mo_{50}V_{50}$	S	0.92	±0.64	-	0.92		
	S-1	−0.19	±0.01	−0.13	−0.17	−1.6	−1.5
	S-2	−0.07	0.00	−0.004	−0.06		
$Mo_{75}V_{25}$	S	1.20	±0.84	-	1.20		
	S-1	−0.36	±0.03	−0.23	−0.25	−4.0	−3.8
	S-2	−0.05	0.00	0.01	−0.04		

TABLE V. Layer-resolved local magnetic moments on V and Mo atoms (in μ_B) for ferromagnetic samples, disordered local moments on V atoms (V_{DLM} in μ_B), energy differences between the ferromagnetic and the nonmagnetic solutions ΔE_{FM-NM} and between the ferromagnetic solution and the solution with a local moments disorder ΔE_{FM-DLM} (in mRy), and deviations of interlayer distances from ideal values of the truncated bcc lattice, i.e., surface relaxation (in %) for the V monolayer deposited at the (100) surface of bcc Mo. Layers are numbered starting with the surface layer S, and decreasing numbers correspond to deeper subsurface layers.

	Layer	V	V_{DLM}	Mo	ΔE_{FM-NM}	ΔE_{FM-DLM}	Surface relaxation
V/Mo(100)	S	1.61	±1.33	-			0
(LMTO-ASA+M,	S-1	-	-	−0.28	−10.2	−8.4	0
unrelaxed)	S-2	-	-	−0.07			0
V/Mo(100)	S	1.68	-	-			0
(VASP,	S-1	-	-	−0.29	−11.65	-	0
unrelaxed)	S-2	-	-	−0.02			0
V/Mo(100)	S	1.41	±0.85	-			−7
(LMTO-ASA+M,	S-1	-	-	−0.27	−5.32	−5.30	0
relaxed)	S-2	-	-	0.07			0
V/Mo(100)	S	1.12	-	-			−6.70
(VASP,	S-1	-	-	−0.21	−3.16	-	−1.43
relaxed)	S-2	-	-	−0.04			−0.35

quite large, and we expect therefore that the Curie temperature may also be higher for the alloys with quenched segregation profiles.

E. Magnetization of a V monolayer deposited at a (100) Mo substrate

Extrapolating our results for segregated surfaces of random V-Mo alloys towards zero concentration of V in the bulk, we expect that the highest value of the magnetic moment, as well as the most stable ferromagnetic solution, may be achieved for a V monolayer deposited on the (100) surface of pure bcc Mo. Therefore, we have carried out calculations for a V monolayer on a Mo substrate, and the results confirm our expectations. In Table V we show local magnetic moments on V atoms in the monolayer, as well as induced moments on Mo atoms in the near-surface region of Mo matrix. Quite clearly, the surface moment reaches the maximal value among the all systems considered in our study, and the stability of the FM solution is also the highest in comparison with the nonmagnetic solution, as well as with the DLM solution. These results are in agreement with electronic structure calculations. According to them, the Fermi energy is located almost exactly at the peak of the surface DOS of a V monolayer. Remember that we calculate nonmagnetic DOS in order to explain our results in terms of the Stoner model.

In order to investigate the effect of magnetic splitting on the surface DOS we have calculated the electronic structure of the ferromagnetic V monolayer on the (100) surface of bcc Mo. The result is shown in Fig. 4. One can see that the peak of the DOS associated with the surface states in the pseudogap is spin split, and the Fermi energy located in the DOS valleys for the both majority- and minority-spin channels. Comparison between the nonmagnetic DOS and FM DOS indicates the instability of the nonmagnetic solution for a V monolayer on a Mo (100) surface. This is confirmed by the high calculated absolute value of the energy difference between the FM and NM solutions for the monolayer case, which is about 3 times higher than that for bulk fcc Ni.[42] A very high absolute value is also calculated for $\Delta E_{FM} - E_{DLM}$. Thus, we predict that experimental verification of our theoretical results should be most straightforward for this particular case. Note that the V monolayer should be relatively stable at the surface, as the surface segregations push V on the top of Mo even for Mo-rich alloys. Also, it is

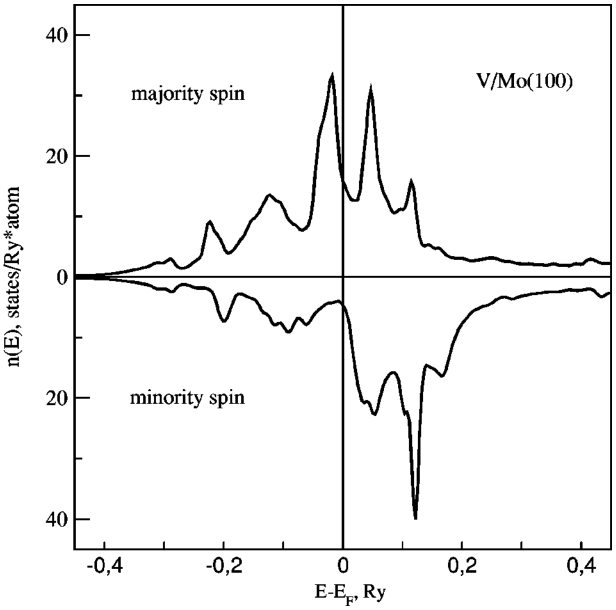

FIG. 4. Vanadium local densities of states $n(E)$ for the *ferromagnetic* V overlayer deposited at the (100) surface of pure bcc Mo. The LDOS is plotted as a function of energy E (relative to the Fermi energy E_F).

known that high-quality V-Mo multilayers can be prepared experimentally.[14,53] Of course, one must take care of the samples to prevent a contamination of the surface—e.g., V oxidation.

At the same time, there are other competing mechanisms, except magnetism, that could reduce the DOS at E_F. For example, one can expect that the surface relaxations will favor the nonmagnetic solution. In order to check if the ferromagnetism is still stable in the presence of surface relaxations, we carried out calculations for a V monolayer on Mo where the interlayer distances were relaxed. For the determination of relaxed geometries we carried out calculations using the supercell technique and the VASP package as described in Sec. II.

In Table V we show the results of our supercell calculations for unrelaxed and relaxed supercells. The results calculated without lattice relaxations compare favorably with our LMTO-ASA+M results. We find that the surface V layer exhibits 6.7% inwards relaxation, which is the same value as the inwards relaxation found experimentally at the (100) surface of pure bcc V.[54] We have calculated the magnetic moments and energy differences between different magnetic solutions for a V monolayer at a Mo substrate with relaxed geometries using both VASP-PAW and LMTO-ASA+M methods. In the latter case we did not determine the relaxations self-consistently. Rather, on the basis of the full-potential calculations we simply have decreased the distance between the surface and first subsurface layer by 7%. The results obtained by means of the two different techniques agree well with each other. One can see from Table V that the surface relaxations reduce the V moments. It also substantially reduces the absolute value of the energy differences between the FM and NM solutions, as well as between the FM and DLM solutions. At the same time, both the magnetic moment and $\Delta E_{FM}-E_{NM}$ ($\Delta E_{FM}-E_{DLM}$) are still quite high. We therefore believe that the V monolayer on the top of a Mo (100) surface should be magnetic.

IV. CONCLUSIONS

In order to investigate the magnetic properties of the bcc (100) surface in the Mo-V system we have carried out *ab initio* simulations for pure V, disordered $\mathrm{Mo}_{25}\mathrm{V}_{75}$, $\mathrm{Mo}_{50}\mathrm{V}_{50}$, and $\mathrm{Mo}_{75}\mathrm{V}_{25}$ alloys, and for a V monolayer deposited on a Mo substrate. Calculations were carried out for uniformly random alloys, as well as for alloys with self-consistent segregation profiles quenched from high temperatures. The main results are the following.

(i) While the MoV alloy is nonmagnetic in bulk in the whole range of concentrations its (100) surface is magnetic. Noticeable magnetization occurs only at the top surface layer, and in the case of uniformly random alloys the total surface magnetization slightly decreases with increasing Mo concentration.

(ii) Vanadium segregates strongly towards the (100) surface. Even in the case of the $\mathrm{Mo}_{75}\mathrm{V}_{25}$ alloy the surface is almost completely covered by V.

(iii) The vanadium segregation towards the surface leads to a little drop in magnetization for the $\mathrm{Mo}_{25}\mathrm{V}_{75}$ alloy, but it enhances strongly the surface magnetization, as well as the stability of the ferromagnetic solution for Mo-rich alloys.

(iv) We predict that the most stable magnetic moments can be found in the case of a V monolayer deposited on a (100) surface of pure Mo. The ferromagnetic solution in this system is stable both with respect to local moment disorder and surface relaxations.

(v) The onset of magnetization on the (100) surface in the Mo-V system is explained by a successive shift of V surface states pinned in an alloy pseudogap towards the Fermi level by a filling of the bulk *d* band by electrons due to alloying of V with Mo.

ACKNOWLEDGMENTS

The authors would like to acknowledge useful discussions with Dr. I. Turek, Dr. D. Arvanitis, Dr. O. Karis, Professor M. I. Katsnelson, and Professor B. Hjörvarsson. The collaboration between Sweden and the former Soviet Union was supported by The Royal Swedish Academy of Sciences (KVA). We are grateful to the Swedish Research Council (VR) and the Swedish Foundation for Strategic Research (SSF) for financial support. E.I.I and Yu.Kh.V. would like to thank the Netherlands Organization for Scientific Research (Grant No. 047-008-016) and the Russian Foundation for Basic Researches (Grant No. 01-02-16156) for financial support.

---

[1] P. Grünberg, R. Schreiber, Y. Pang, M.B. Brodsky, and H. Sowers, Phys. Rev. Lett. **57**, 2442 (1986).

[2] S.S.P. Parkin, N. More, and K.P. Roche, Phys. Rev. Lett. **64**, 2304 (1990).

[3] M.N. Baibich, J.M. Broto, A. Fert, F. Nguyen van Dau, F. Petroff, P. Eitenne, G. Creuzet, A. Friederich, and J. Chazelas, Phys. Rev. Lett. **61**, 2472 (1988).

[4] H. Ohno, Science **281**, 951 (1998); Y. Ohno *et al.*, Nature (London) **407**, 790 (1999); H. Ohno *et al.*, *ibid.* **408**, 944 (2000).

[5] A.J. Freeman and R. Wu, J. Magn. Magn. Mater. **104–107**, 1 (1992).

[6] I. Morrison, D.M. Bylander, and L. Kleinman, Phys. Rev. Lett. **71**, 1083 (1993).

[7] M. Weinert, S. Blügel, and P.D. Johnson, Phys. Rev. Lett. **71**, 4097 (1993).

[8] J.-H. Cho and M. Scheffler, Phys. Rev. Lett. **78**, 1299 (1997).

[9] S. Blügel, Europhys. Lett. **18**, 257 (1992).

[10] C. Rau, C. Liu, A. Schmalzbauer, and G. Xing, Phys. Rev. Lett. **57**, 2311 (1986).

[11] M. Stampanoni, Appl. Phys. A: Solids Surf. **49**, 449 (1989).

[12] R.L. Fink, C.A. Ballentine, and J.L. Erskine, Phys. Rev. B **41**, 10 175 (1990).

[13] C. Binns, H.S. Derbyshire, S.C. Bayliss, and C. Norris, Phys. Rev. B **45**, 460 (1992).

[14] V. Korenivski, K.V. Rao, J. Birch, and J.-E. Sundgren, J. Magn.

Magn. Mater. **140–144**, 523 (1995).

[15] C.L. Fu, A.J. Freeman, and T. Oguchi, Phys. Rev. Lett. **54**, 2700 (1985).

[16] A.J. Freeman and C.L. Fu, J. Appl. Phys. **61**, 3356 (1987).

[17] G. Bihlmayer, T. Asada, and S. Blügel, Phys. Rev. B **62**, 11 937 (2000).

[18] T. Bryk, D.M. Bylander, and L. Kleinman, Phys. Rev. B **61**, R3780 (2001).

[19] I.G. Batyrev, J.-H. Cho, and L. Kleinman, Phys. Rev. B **63**, 172420 (2001).

[20] R. Robles, J. Izquierdo, A. Vega, and L.C. Balbas, Phys. Rev. B **63**, 172406 (2001).

[21] S. Blügel and P. Dederichs, Europhys. Lett. **9**, 597 (1987).

[22] M.J. Zhu, D.M. Bylander, and L. Kleinman, Phys. Rev. B **43**, 4007 (1991).

[23] O. Eriksson, R.C. Alders, and A.M. Boring, Phys. Rev. Lett. **66**, 1350 (1991).

[24] M. Stampanoni, A. Vaterlaus, D. Pescia, M. Aeschlimann, F. Meier, W. Dürr, and S. Blügel, Phys. Rev. B **37**, 10 380 (1988).

[25] C. Rau, G. Xing, and M. Robert, J. Vac. Sci. Technol. A **6**, 579 (1988).

[26] R.L. Fink, C.A. Ballentine, J.L. Erskine, and J.A. Araya-Pochet, Phys. Rev. B **41**, 10 175 (1990).

[27] S.E. Weber, B.K. Rao, P. Jena, V.S. Stepanyuk, W. Hergert, K. Wildberger, R. Zeller, and P.H. Dederichs, J. Phys.: Condens. Matter **9**, 10739 (1997).

[28] H. Dreysse, A. Vega, C. Demangeat, and L.C. Balbas, Europhys. Lett. **27**, 165 (1994).

[29] I. Turek, S. Blügel, and J. Kudrnovsky, Phys. Rev. B **57**, 11 065 (1998).

[30] *Binary Alloy Phase Diagrams*, edited by T. B. Massalski (American Society for Metals, Metals Park, OH, 1986).

[31] A.V. Ponomareva, L.V. Pourovskii, E.I. Isaev, Yu.Kh. Vekilov, I.A. Abrikosov, and B. Johansson, Phys. Low-Dimens. Semicond. Struct. **1–2**, 347 (2002); A.V. Ponomareva, L.V. Pourovskii, E.I. Isaev, Yu.Kh. Vekilov, B. Johansson, and I.A. Abrikosov, J. Magn. Magn. Mater. **258-259**, 128 (2003).

[32] H.L. Skriver and N.M. Rosengaard, Phys. Rev. B **46**, 7157 (1992).

[33] L. Vitos, A.V. Ruban, H.L. Skriver, and J. Kollar, Surf. Sci. **411**, 186 (1998).

[34] I. Turek (private communication).

[35] H.L. Skriver and N.M. Rosengaard, Phys. Rev. B **43**, 9538 (1991).

[36] I.A. Abrikosov and H.L. Skriver, Phys. Rev. B **47**, 16 532 (1993).

[37] A.V. Ruban and H.L. Skriver, Comput. Mater. Sci. **15**, 119 (1999).

[38] L.V. Pourovskii, A.V. Ruban, I.A. Abrikosov, Yu.Kh. Vekilov, and B. Johansson, Phys. Rev. B **64**, 035421 (2001).

[39] A.V. Ruban and H.L. Skriver, Phys. Rev. B **66**, 024201 (2002); A.V. Ruban, S.I. Simak, P.A. Korzhavyi, and H.L. Skriver, *ibid.* **66**, 024202 (2002).

[40] L.V. Pourovskii, A.V. Ruban, I.A. Abrikosov, Yu.Kh. Vekilov, and B. Johansson, JETP Lett. **73**, 415 (2001).

[41] S.H. Vosko, L. Wilk, and M. Nusair, Can. J. Phys. **58**, 1200 (1980).

[42] E.I. Isaev, L.V. Pourovskii, A.M.N. Niklasson, Yu.Kh. Vekilov, B. Johansson, and I.A. Abrikosov, Phys. Rev. B **65**, 024435 (2002).

[43] J.M. Sanchez, F. Ducastelle, and D. Gratias, Physica A **128**, 334 (1984).

[44] A.V. Ruban, I.A. Abrikosov, D.Ya. Kats, D. Gorelikov, K.W. Jacobsen, and H.L. Skriver, Phys. Rev. B **49**, 11 383 (1994).

[45] W. Schweika and A.E. Carlson, Phys. Rev. B **40**, 4990 (1989).

[46] G. Kresse and J. Furthmüller, Comput. Mater. Sci. **6**, 15 (1996); Phys. Rev. B **54**, 11 169 (1996).

[47] G. Kresse and J. Joubert, Phys. Rev. B **59**, 1758 (1999).

[48] P.E. Blöchl, Phys. Rev. B **50**, 17 953 (1994).

[49] P.E. Blöchl, O. Jepsen, and O.K. Andersen, Phys. Rev. B **49**, 16 223 (1994).

[50] P.H. Citrin and G.K. Wertheim, Phys. Rev. B **27**, 3176 (1983).

[51] L.V. Pourovskii, N.V. Skorodumova, Yu.Kh. Vekilov, B. Johansson, and I.A. Abrikosov, Surf. Sci. **439**, 111 (1999).

[52] I.A. Abrikosov, P. James, O. Eriksson, P. Söderlind, A.V. Ruban, H.L. Skriver, and B. Johansson, Phys. Rev. B **54**, 3380 (1996).

[53] G. Håkansson, J. Birch, L. Hultman, I.P. Ivanov, J.-E. Sundgren, and R. Wallenberg, J. Cryst. Growth **121**, 399 (1992).

[54] D.L. Adams, H.B. Nielsen, and J.N. Andersen, Phys. Scr. **T4**, 22 (1983).